Published in final edited form as:
Free Radic Biol Med. 2012 September 1; 53(5): 1123–1138. doi:10.1016/j.freeradbiomed.2012.05.036.

Mitochondrial reactive oxygen species generation triggers inflammatory response and tissue injury associated with hepatic ischemia-reperfusion: therapeutic potential of mitochondrially-targeted antioxidants

Partha Mukhopadhyay[1,*], **Bėla Horváth**[1,*], **Zsuzsanna Zsengellėr**[3,*], **Sándor Bátkai**[1,*], **Zongxian Cao**[1], **Malek Kechrid**[1], **Eileen Holovac**[1], **Katalin Erdėlyi**[1], **Galin Tanchian**[1], **Lucas Liaudet**[4], **Isaac E. Stillman**[3], **Joy Joseph**[2], **Balaraman Kalyanaraman**[2], and **Pál Pacher**[1]

[1]Laboratory of Physiologic Studies, National Institute on Alcohol Abuse and Alcoholism, National Institutes of Health, Bethesda, Maryland, USA [2]Free Radical Research Center, Medical College of Wisconsin, Milwaukee, Wisconsin 53226 [3]Department of Pathology, Beth Israel Deaconess Medical Center, and Harvard Medical School, Boston, Massachusetts 02215, USA [4]Department of Intensive Care Medicine, University Hospital Center and Faculty of Biology and Medicine, 1011 Lausanne, Switzerland

Abstract

Mitochondrial reactive oxygen species generation has been implicated in the pathophysiology of ischemia-reperfusion (I/R) injury, however its exact role and its spatial-temporal relationship with inflammation are elusive. Herein we explored the spatial-temporal relationship of oxidative/nitrative stress and inflammatory response during the course of hepatic I/R and the possible therapeutic potential of mitochondrial-targeted antioxidants, using a mouse model of segmental hepatic ischemia-reperfusion injury. Hepatic I/R was characterized by early (at 2 hours of reperfusion) mitochondrial injury, decreased complex I activity, increased oxidant generation in the liver or liver mitochondria, and profound hepatocellular injury/dysfunction with acute pro-inflammatory response (TNF-α, MIP-1αCCL3, MIP-2/CXCL2) without inflammatory cell infiltration, followed by marked neutrophil infiltration and more pronounced secondary wave of oxidative/nitrative stress in the liver (starting from 6 hours of reperfusion and peaking at 24 hours). Mitochondrially-targeted antioxidants, MitoQ or Mito-CP, dose-dependently attenuated I/R-induced liver dysfunction, the early and delayed oxidative and nitrative stress response (HNE/carbonyl adducts, malondialdehyde, 8-OHdG, and 3-nitrotyrosine formation), mitochondrial and histopathological injury/dysfunction, as well as delayed inflammatory cell infiltration and cell death.

Mitochondrially generated oxidants play a central role in triggering the deleterious cascade of events associated with hepatic I/R, which may be targeted by novel antioxidants for therapeutic advantage.

Corresponding Author: Pál Pacher M.D., Ph.D., F.A.P.S., F.A.H.A., F.A.C.C., Section on Oxidative Stress Tissue Injury, Laboratory of Physiological Studies, National Institutes of Health/NIAAA, 5625 Fishers Lane, MSC-9413, Bethesda, Maryland 20892-9413, USA., Phone: (301)443–4830; Fax: (301)480–0257; pacher@mail.nih.gov.
*equally contributed

Keywords

ischemia-reperfusion; antioxidants; oxidative stress; reactive oxygen and nitrogen species

Introduction

Ischemia-reperfusion (I/R) inflicted by transient ischemia followed by reperfusion is a pivotal mechanism of organ injury during various pathological conditions (e.g. myocardial infarction, stroke, vascular surgeries, circulatory shock, and organ transplantation). Surgical interventions in the liver, transplantation, inflammatory and vascular diseases, circulatory shock or various toxic insults may lead to hepatic I/R injury resulting in organ dysfunction or failure, depending on the duration of the insult [1–3]. Early generation of reactive oxygen (e.g. superoxide and hydrogen peroxide) and nitrogen (e.g. peroxynitrite) species (ROS/RNS) during reperfusion is considered playing a pivotal role in initiating a chain of deleterious cellular responses leading to inflammation and cell death, which eventually culminate in target organ dysfunction/failure [3–11]. Mitochondrial proteins are particularly sensitive targets for ROS/RNS [12], and their inactivation by oxidants may contribute to dysfunction and injury during hepatic [13] and other forms of liver injury [14]. Dysfunctional mitochondria may also generate significant amount of ROS during hepatic I/R in addition to activated xanthine oxidoreductases, NADPH oxidases in various key cell types of the liver (e.g. hepatocytes, endothelial, Kupffer, and infiltrating immune cells) [15–17].

Despite numerous reports on the role of oxidative stress and mitochondrial dysfunction in hepatic I/R injury, and on the beneficial effects of global antioxidants, the exact role of mitochondrial ROS generation in liver I/R injury is still largely elusive. Furthermore, there is very limited information on the spatial-temporal relationship of the oxidative and nitrative stress and inflammatory response during hepatic I/R, and on the main cellular sources/targets of ROS/RNS generation. In this study, we used a well-established mouse model of in vivo segmental hepatic I/R injury [13, 18–20] and two well-characterized mitochondrially-targeted small-molecule antioxidants, MitoQ and Mito-CP [21–24], to investigate the role of oxidative stress and mitochondrial oxidant generation during the course of hepatic I/R.

Materials and methods

Hepatic ischemia-reperfusion

The study has been approved by the Institutional Animal Care and Use Committees of NIAAA, and has been carried out in line with the National Institutes of Health (NIH) guidelines for the care and use of laboratory animals. Male C57BL/6J mice (25–30g; Jackson Laboratories, Bar Harbor, ME) were anesthetized with pentobarbital sodium (65 mg/kg i.p.). In our study, the model of segmental (70%) hepatic ischemia-reperfusion has been used, as described [13, 18–20, 25, 26]. Two mitochondrially-targeted antioxidants, which most likely inhibit lipid peroxidation and also quench peroxynitrite, Mito-Q and Mito-CP were synthesized as described [21, 27]. MitoQ and Mito-CP were stored in ethanol at 50 mg/ml, further diluted in saline and administered at 0.3–3 mg/kg or as described, i.p. once, 1.5 hour before I/R. Mito-Q and Mito-CP at 3 mg/kg or vehicle were also given right after the ischemia at the moment of reperfusion (post I (R 0h)) or 3h after ischemia (post I (R 3h)), as indicated in the text. At the experimental end points at 2, 6 and 24 hours following ischemia (I/R 2, 6 and 24h), blood was collected and liver samples were removed and snap-frozen in liquid nitrogen for determining biochemical parameters or fixed in 4% buffered formalin for histopathological evaluation.

Serum AST and ALT levels

The activities of aspartate amino-transferase (AST) and alanine amino-transferase (ALT), indicators of liver cellular damage, were measured in serum samples using a clinical chemistry analyzer system (VetTest 8008, IDEXX laboratories, Westbrook, ME) [13, 19].

Histological examination of liver sections

Liver samples were fixed in 4% buffered formalin. After embedding and cutting 5 μm slices, all sections were stained with hematoxylin/eosin (HE). Myeloperoxidase staining of neutrophils was done by using anti-myeloperoxidase antibody according to the manufacturer's protocol (Biocare Medical, Concord, CA), and samples were counter-stained with nuclear fast red as described [19]. Liver sections were also stained for malondialdehyde (Genox Corporation, Baltimore, MD), nitrotyrosine (Cayman Chemical, Ann Arbor, MI) and 8-hydroxy-2′-deoxyguanosine (8-OHdG) (Genox Corporation, Baltimore, MD) according to the manufacturer's protocol and/or as described [20, 28]. Both malondialdehyde and nitrotyrosine stained sections were counter stained with nuclear fast red. The specific staining was visualized and images were acquired using microscope IX-81 with 20X, 40X and 100x objectives (Olympus, Center Valley, PA) [20, 28]. Histological evaluation was performed in a blinded manner.

Electron Microscopy

Livers of anesthetized animals were perfusion fixed with 1.25 % glutaraldehyde in 0.1 M cacodylate buffer. Livers were harvested and processed in standard fashion (Epon embedded) for transmission electron microscopy using a JEOL 1011 Electron Microscope as described [28].

Real-Time PCR Analyses of mRNA

Total RNA was isolated from liver homogenate using TRIzol reagents (Invitrogen, Carlsbad, CA) according to manufacturer's instructions. The isolated RNA was treated with RNase-free DNase (Ambion, Austin, TX) to remove traces of genomic DNA contamination. One microgram of total RNA was reverse-transcribed to cDNA using the SuperScript II (Invitrogen, Carlsbad, CA). The target gene expression was quantified with Power SYBER Green PCR Master Mix using an ABI HT7900 real-time PCR instrument (Applied Biosystems, Foster City, CA). Each amplified sample in all wells was analyzed for homogeneity using dissociation curve analysis. Relative quantification was calculated using the comparative CT method.

All primers used were previously described [20, 26, 29, 30]:

TNF-α, 5′-AAGCCTGTAGCCCACGTCGTA-3′ and 5′-AGGTACAACCCATCGGCTGG-3′; MIP-1α, 5′-TGCCCTTGCTGTTCTTCTCTG-3′ and 5′-CAACGATGAATTGGCGTGG-3′; MIP-2, 5′-AGTGAACTGCGCTGTCAATGC-3′ and 5′-AGGCAAACTTTTTGACCGCC-3′; gp91Phox (NOX2), 5′-GACCATTGCAAGTGAACACCC-3′ and 5′-AAATGAAGTGGACTCCACGCG-3′; and actin, 5′-TGCACCACCAACTGCTTAG-3′ and 5′-GGATGCAGGGATGATGTTC-3′.

Immunoblot analyses

Liver tissues were homogenized in mammalian tissue protein extraction reagent (Pierce, Rockford, IL, USA) supplemented with protease and phosphatase inhibitors (Roche Diagnostics) Blots were probed with gp91phox (BioLegend Inc, San Diego, CA) used at 1:1000 dilution and incubated overnight at 4 C. After subsequent washing with PBS–Tween, the membranes were probed with appropriate secondary antibodies conjugated with HRP

(Pierce, Rockford, IL) and incubated 1h at room temperature. Then the membranes were developed using a SuperSignal–West Pico substrate chemiluminescence detection kit (Pierce, Rockford, IL). To confirm uniform loading, membranes were stripped and re-probed with β-actin (Chemicon, Ramona, CA, USA).

Isolation of Mitochondrial fraction

Mitochondria were isolated from the livers of mice treated with vehicle, or Mito-CP/MitoQ with or without exposure to I/R using tissue mitochondrial isolation kit (Pierce Biotechnology, Rockford, IL) as decribed [20].

Determination of mitochondrial complex activity

Microplate assay kits (MitoSciences, Inc., Eugene, OR, USA) were used to determine the activity of Mitochondrial complex I, complex II and complex IV according to the manufacturer's instructions. The complex enzymes were immunocaptured within the wells of the microplate and activities were determined colorimetrically. Complex activities were expressed as percentage activity compared to the liver samples of the vehicle-treated mice as described [20].

Hepatic and/or mitochondrial 4-hydroxynonenal (HNE) content and protein oxidation

Lipid peroxides are unstable indicators of oxidative stress in cells that decompose to form more complex and reactive compounds such as 4-hydroxynonenal (HNE), which has been shown to be capable of binding to proteins and forming stable HNE adducts. HNE adducts in the hepatic tissues or from mitochondrial fractions were determined using a kit (Cell Biolabs, San Diego, CA). In brief, BSA or hepatic tissue extracts (10 μg/mL) were adsorbed onto a 96-well plate. HNE adducts present in the sample or standard were probed with anti-HNE antibody, followed by an HRP conjugated secondary antibody. The HNE-protein adducts content in an unknown sample was determined by comparing with a standard curve.

The protein oxidation was also determined in isolated mitochondrial fractions by OxyBlot Protein Detection Kit from EMD Millipore (Billerica, MA) according to manufacturer instructions. This method is based on the immunoblot detection of carbonyl groups introduced into proteins by oxidative reactions with ozone or oxides of nitrogen or by metal catalyzed oxidation.

Mitochondria for oxyblot analyses were purified by magnetic beads method (Mitochondria Isolation Kit, Miltenyi Biotec, Auburn, CA) as described earlier [31]. The isolation of mitochondria was carried out according to manufacturer's instruction. Briefly, fresh harvested liver was homogenized by gentleMACS dissociator (Miltenyi Biotec, Auburn, CA). To magnetically label mitochondria, the homogenate was incubated with 50 μl of monoclonal anti-TOM22-conjugated microBeads for 1 hour at 4°C. Then, the suspension of labeled mitochondria was loaded onto a pre-equilibrated MACS Column (Miltenyi Biotec, Auburn, CA), previously placed in the magnetic field of a MACS Separator (Miltenyi Biotec, Auburn, CA). Due to the magnetic field generated by the MACS Separator, labeled-mitochondria were retained into the column. The column was washed three times with 3 ml suspension buffer provided with the kit. Subsequently, the column was removed from the magnetic field and the retained mitochondria were eluted in 1 ml suspension buffer. The mitochondrial lysates were prepared in RIPA buffer and the purity of mitochondrial fraction was analyzed by western blot with cytochrome c oxidase (COX IV) antibody (Abcam, Cambridge, MA).

Hepatic protein carbonyl content

Protein oxidation is defined as the covalent modification of the proteins induced by reactive oxygen species. Oxidative modification of proteins can be induced by wide array of pro-oxidant stimulus, and elevated levels were demonstrated in several pathological conditions. An ELISA-based assay (Cell Biolabs Inc., San Diego, CA) was used to measure the protein carbonyl levels in isolated liver mitochondrial fractions. In brief, BSA standards or protein samples were adsorbed on to 96-well plates for 2 h at 37°C. The protein carbonyls present in the samples or standards were derivatized to DNP hydrazones with dinitrophenylhydrazine (DNPH) and incubated with anti-DNP antibody, followed with HRP conjugated secondary antibody. Then the absorbance was measured at 450 nm using a plate reader (Spectramax Plus, Molecular Device, Sunnyvale, CA) as described [32, 33]..

Hepatic 3-nitrotyrosine (NT) content

NT content was measured by the NT ELISA kit from Hycult Biotechnology (Cell Sciences, Canton, MA) from tissue homogenates as described [20, 33]. Levels were presented as fold changes compared to vehicle-treated control sample.

Hepatic DNA fragmentation and poly (ADP-ribose) polymerase (PARP) activity

The quantitative determinations of cytoplasmic histone-associated-DNA-fragmentation (mono and oligonucleosomes) due to cell death in liver homogenizates were measured using ELISA kit (Roche Diagnostics GmbH, Indianapolis, IN)[34]. Hepatic PARP activity was assayed using a colorimetric kit according to the manufacturer's protocol (Trevigen, Gaithersburg, MD) as described [20].

Analysis of data

Results are expressed as means ± SEM. Statistical significance among groups was determined by one-way ANOVA followed by Newman-Keuls post hoc analysis using GraphPad Prism 5 software (San Diego, CA). Probability values of $P<0.05$ were considered significant.

Results

Mitochondrially-targeted antioxidants attenuate markers of hepatic I/R injury (ALT, AST) and histological damage

After 1 hour of ischemia and a subsequent 2 or 6 hours of reperfusion (I/R 2 h or I/R 6h), a dramatic increase in the serum transaminase enzyme activities (AST and ALT; markers of hepatocellular damage/necrosis) were observed in vehicle-treated C57BL/6J mice (peaking at 6h of reperfusion), as compared with sham-operated controls (Figure 1B–D). At 24 hours of reperfusion (I/R 24h) the transaminase activities declined compared I/R 6h, but were still elevated compared to sham-operated controls (Figure 1D). Pretreatment with MitoQ or Mito-CP (Figure 1A) (0.3–3 mg/kg i.p.) 1.5 hours before the induction of the ischemia dose-dependently attenuated the serum transaminase elevations at 6 hours of reperfusion compared to vehicle (Figure 1B–C). MitoQ or Mito-CP (3 mg/kg i.p.) 1.5 hours before the induction of the ischemia significantly attenuated the serum transaminase elevations at 2, 6, and 24 hours of reperfusion compared to vehicle (Figure 1D). MitoQ and Mito-CP (3 mg/kg i.p.) were also effective in attenuating the I/R-induced peak ALT/AST elevations at 6 h of reperfusion when administered right after the 1 h ischemic period before the start of the reperfusion (Figure 2A; post I (R 0h)), however they lost their protective effects on liver dysfunction when administered at 3 hours of reperfusion (Figure 2B; post I (R 3h)).

We hypothesized that the mitochondrial dysfunction/ROS generation triggers the deleterious cascade of events during I/R (e.g. secondary inflammatory response and ROS/RNS generation, etc.), therefore we studied mitochondrial structure early at 2 h of reperfusion. The electron microscopy of the non-ischemic control livers of mice undergoing sham surgery (sham) revealed normal hepatic tissue with good preservation of hepatocytes and lining cells of sinusoidal venules, as well as normal mitochondrial structure (Figure 3A, left panels), which were similar in sham mice treated with MitoQ or Mito-CP (3 mg/kg i.p.) (Figure 3A middle and right panels).

Post-ischemic liver tissue at 2 hours of reperfusion (I/R 2h) exhibited marked disintegration of ultrastructure (e.g., swelling of mitochondria, vacuolization, nuclear and cytoplasmic degeneration) in most hepatocytes (Figure 3B, left panels). The majority of mitochondria exhibited alterations in size, shape, and matrix. In some mitochondria the matrix totally disappeared and only the outer membrane remained, while in others, the cristae appeared disorganized because of edema in the matrix, and many of them lost the spherical or ellipsoid shape (Figure 3B, left panels). Mito-CP and MitoQ pretreatment (3 mg/kg i.p.) markedly attenuated the morphological and mitochondrial injury induced by 1 h of ischemia followed by 2 hours of reperfusion (I/R 2h) to a similar extent (Figure 3B, middle and right panels).

Representative liver sections of sham mice, mice exposed to 1 hour of ischemia followed by 2, 6 and 24 hours of reperfusion (I/R) with vehicle or Mito-CP/MitoQ pretreatment were stained with hematoxylin and eosin (Figure 4). The I/R-induced marked coagulation necrosis was histologically clearly separated by 6 and 24h of I/R (lighter areas, with marked inflammatory cell infiltration at 24 hours of reperfusion), which was dramatically reduced and became more focal in Mito-CP/MitoQ treated mice (Figure 4). Mito-CP/MitoQ treatment alone or vehicle had no effect on the liver histopathology. Figure 4 depicts 200× magnifications.

Mitochondrially-targeted antioxidants attenuate the I/R-induced oxidative and nitrative stress, and mitochondrial dysfunction in the liver

The rate of hepatic lipid peroxidation (HNE; Figure 5A) was negligible in sham-operated mouse liver as indicated by the low levels of HNE adducts. Hepatic HNE adducts time-dependently increased at 2, 6 and 24 hours of reperfusion, and were markedly attenuated by mitochondrial antioxidants (Figure 5A). Consistently with early mitochondrial injury (Figure 3) and ROS/RNS formation (Figure 5A–D), the level of hepatic and mitochondrial HNE adducts (Figure 5A and B) and oxidized proteins (protein carbonyl adducts; Figure 5C and D) were elevated at 2 h of reperfusion. Marked attenuation of mitochondrial complex I activity was also observed at 2h of reperfusion, without significant changes in complex II and IV activities (Figure 5E).

Mitochondrial antioxidants almost completely prevented the I/R-induced early elevation of HNE and/or protein oxidation in the mitochondria (Figure 5A–D), as well as attenuated the impaired complex I activity measured from isolated liver mitochondria (Figure 5E, left panel). These data indicate that mitochondria represent the primary source of ROS generation during early reperfusion injury and Mito-CP/MitoQ is able to selectively target ROS in these organelles.

24 hours of I/R also induced marked increases in liver malondialdehyde formation (another index of lipid peroxidation; brown staining), which was predominantly localized to endothelial cells, perivascular hepatocytes, and infiltrating (or attached to the endothelium) inflammatory cells (Figure 6A, second pair of images from the left). Mitochondrial antioxidants markedly attenuated the I/R-induced malondialdehyde formation in the liver

(Figure 6A, 2 pairs of images from the right). Similar pattern but weaker staining (without infiltrating immune cells) was observed at earlier time points (I/R 2 and 6h; data not shown). Minimal staining could be seen in the livers of control mice exposed to sham surgery (Figure 6A, left panels).

24 hours of I/R was also associated with increased 8-OHdG formation (a marker of oxidative DNA injury; strong dark blue nuclear staining) in endothelial cells, perivascular hepatocytes and infiltrating inflammatory cells (Figure 6B, second pair of images from the left). Mitochondrial antioxidants markedly attenuated the I/R-induced 8-OHdG formation in the liver (Figure 6B, 2 pairs of images from the right). Minimal nuclear 8-OHdG staining could be seen in the livers of control mice exposed to sham surgery (Figure 6B, left panels). The upper row of images (Figures 6A and B) depicts 400× magnification, the lower 1000×.

Consistently with previous studies [16, 20] from 6 h of reperfusion there was an increased expression (mRNA and/or protein) of ROS generating NADPH oxidase isoform NOX2/gp91phox in the liver, coinciding with the inflammatory cell infiltration; which were also attenuated by Mito-CP/MitoQ pretreatments (Figure 7A,B). In contrast, when Mito-CP/MitoQ were administered 3 hours after the ischemia they were not able to attenuate the I/R-induced NOX2 protein expression determined at 24 hours of reperfusion (Figure 7C).

I/R was also associated with time-dependent marked increases of hepatic and/or mitochondrial 3-nitrotyrosine formation (Figures 8A–C, and 9), a marker of peroxynitrite formation and more broadly nitrative stress [3]), showing similar cellular localization to malondialdehyde and 8-OHdG in endothelial cells, perivascular hepatocytes, and infiltrating (or attached to the endothelium) inflammatory cells (Figures 6, 8 and 9). Mito-CP/MitoQ markedly attenuated the hepatic/mitochondrial nitrative damage (Figures 8A–C and 9). Figure 8C depicts 400× magnification, Figure 9 depicts 1000×.

Mitochondrially-targeted antioxidants attenuate the I/R-induced acute and delayed inflammatory responses

I/R induced time-dependent changes in the mRNA expression of the pro-inflammatory cytokine tumor necrosis factor α (TNF-α), chemokines macrophage inflammatory proteins 1α and 2 (MIP-1α/CCL3 and MIP2/CXCL2), intercellular adhesion molecule 1 (ICAM-1/CD54) (Figures 10, and 11A), and hepatic myeloperoxidase activity and staining (an indicator of leukocyte infiltration; Figure 11B-D). The I/R-induced acute hepatic pro-inflammatory response (TNF-α, MIP-1α/2, ICAM-1; most likely orchestrated by activated Kupffer and endothelial cells [20, 35] peaked at 2 hours of reperfusion and was largely declined thereafter by 24 hours of reperfusion (Figures 10 and 11A). In contrast, the delayed inflammatory cell (predominantly myeloperoxidase positive neutrophil (brown staining)) infiltration started only from 6 hours of reperfusion peaking at 24 hours of reperfusion (Figures 11C and D). These changes in inflammatory responses were largely attenuated by pre-treatment with Mito-CP/MitoQ (3 mg/kg i.p., Figures 10, and 11A–D). Figure 11C depicts 200× magnification, Figure 11D depicts 400×.

Mitochondrially-targeted antioxidants attenuate the I/R-induced cell death

I/R markedly increased the poly (ADP-ribose) polymerase-dependent (mostly necrotic) and apoptotic (DNA fragmentation, caspase 3/7activity) cell death (Figure 12A–C) in the liver, which were prevented by Mito-CP/MitoQ. Notably, while PARP activity was already increased early following reperfusion (Figure 12A), the apoptotic cell death was evident mainly at 24 h of I/R only (Figure 12B and C).

Discussion

In this study we explored the therapeutic potential of mitochondrially-targeted antioxidants in a well-established mouse model of segmental hepatic ischemia-reperfusion (I/R) injury [13, 18–20, 26]. Previous in vitro, ex vivo, and in vivo studies using this and other models of hepatic I/R have implicated an important role of oxidative/nitrative stress, mitochondrial dysfunction and inflammation in hepatic I/R injury, and demonstrated beneficial effects of various global antioxidants [5, 7, 13, 15, 17, 36]. However, the exact role of mitochondrial ROS generation during liver I/R injury is still largely elusive, likewise the spatial-temporal relationship of the oxidative/nitrative stress and inflammatory cell infiltration. We hypothesized that the I/R-induced mitochondrial oxidative stress results in mitochondrial injury and dysfunction, which may trigger a cascade of deleterious cellular consequences continuously fueling oxidative/nitrative stress, endothelial and hepatocyte cell demise, local inflammation, eventually culminating in liver dysfunction/failure. To test this hypothesis, we administered membrane-permeable small molecule antioxidants that target mitochondria 1.5 hr before I/R challenge and observed marked improvements in each of these pathogenic events including, most importantly, hepatocellular damage. These findings indicate that mitochondrial ROS is a crucial mediator of hepatic I/R injury, which can be selectively targeted by novel antioxidants for therapeutic gain.

The early damaging effect of I/R is caused by the generation of superoxide and other forms of ROS during reperfusion which may involve activation of xathine oxidoreductases [15, 37, 38], impairment of the activities of the enzymes of the mitochondrial respiratory chain, mitochondrial dysfunction, allowing more ROS to leak out of the respiratory chain [6, 13, 20]. Superoxide may also readily react with nitric oxide (NO) during early hepatic reperfusion (the latter can be derived from nitric oxide synthases, most likely iNOS [39]) via a diffusion limited reaction to form a more potent oxidant peroxynitrite [40], further impairing mitochondrial [12] and cellular functions and increasing ROS generation [3, 4]. Hepatic I/R also attenuates endothelial NO synthase activity in sinusoidal endothelial cells during I/R leading to endothelial dysfunction, favoring sinusoidal vasoconstriction. The initial oxidant-induced injury also leads to the activation of endothelial cells and the resident macrophages of the liver, the Kupffer cells [2], which together orchestrate the acute and delayed pro-inflammatory response leading to attraction of neutrophils and other inflammatory cells into the damaged tissue upon reperfusion [2, 20]. These inflammatory cells further release oxidants and proteolytic enzymes enhancing intracellular oxidative/nitrative stress and mitochondrial dysfunction in hepatocytes, thereby promoting apoptotic and/or necrotic, or other forms of cell demise [6, 9, 41].

Increased oxidative/nitrative stress was one of the earliest features we observed during the initial phase of hepatic I/R (I/R 2h) both in the liver, as well as in the isolated liver mitochondria. The above mentioned changes were also accompanied by structural mitochondrial injury in the liver, decreased mitochondrial complex I activity, and hepatocellular necrosis. The early mitochondrial and hepatocellular injury and dysfunction were coupled with an acute pro-inflammatory cytokine/chemokine response (originating from activated Kupffer and endothelial cells) without significant inflammatory cell infiltration. The above mentioned pathological changes were followed by profound delayed neutrophil infiltration and a secondary wave of ROS/RNS generation from 6 hours following ischemia (IR 6 h), peaking at 24 hours of reperfusion (I/R 24h). The later response, consistently with other reports [20], most likely involved the phagocyte NAD(P)H oxidase isoform gp91phox/NOX2 [16], increased iNOS and cyclooxygenase 2 expression[20], and coincided with enhanced leukocyte infiltration in the injured livers. The I/R-induced ROS/RNS generation may also induce expression of adhesion molecules through the activation of NF-κB[18, 20]. Indeed, we found increased expression of adhesion

molecule ICAM-1 in the liver exposed to I/R. This, coupled with the pro-inflammatory cytokines/chemokines released by activated Kupffer and endothelial cells, and possibly certain subpopulations of T cells, may facilitate migration, adhesion and activation of neutrophils to the site of injury, which may further amplify oxidative and nitrative stress, and these processes are interrelated leading to a concerted activation of various mitochondrial and other (e.g. PARP-1-dependent) cell death pathways.

A single dose of mitochondrially-targeted antioxidants, MitoQ/Mito-CP, not only attenuated the I/R-induced liver dysfunction, mitochondrial and hepatic early and delayed oxidative and nitrative stress (HNE/carbonyl adducts, malondialdehyde, 8-OHdG, and nitrotyrosine), mitochondrial and histopathological injury/dysfunction, but also blunted the early and the secondary wave of pro-inflammatory responses and associated cell death. Our results are also in agreement with a recent study demonstrating protective effects of MitoQ against alcohol-induced liver injury, where MitoQ successfully attenuated the alcohol-induced hepatic mitochondrial complex I dysfunction and associated oxidative/nitrative damage [14]. Even though the exact mechanisms of the direct protective effects of MitoQ/Mito-CP are not known, our study supports the view that these antioxidants can attenuate mitochondrial dysfunction and ROS/RNS generation in vivo under pathological conditions, most likely by attenuating lipid peroxidation and/or by quenching peroxynitrite. The most likely primary cellular targets of the protective effects of these compounds against liver I/R injury are the hepatocytes and endothelial cells; however in light of the emerging view that mitochondrial ROS/RNS formation may directly or indirectly control expression of NAD(P)H oxidases [42] and other key processes in various cell types, a direct effect of MitoQ/Mito-CP on early Kupffer cell activation cannot be excluded either. On the other hand, compelling evidence suggests that various molecules released from necrotic hepatocytes during early hepatic I/R (e.g. high mobility group 1 proteins (HMGB1) and DNA fragments), as well as lipid peroxidation products such as hydroxynonenal (HNE), are key triggers of Kupffer cells activation via toll like receptors (TLRs) [2, 43, 44]. Thus, attenuation of early mitochondrial dysfunction, oxidative/nitrative stress, and subsequent necrotic cell death in hepatocytes and endothelial cells during early I/R can also lead indirectly to attenuation of the acute pro-inflammatory response orchestrated by activated Kupffer cells and consequent delayed inflammatory cell infiltration. Figure 13 summarizes the key pathological processes during hepatic I/R injury.

Collectively, these observations strongly indicate that early mitochondrial ROS generation triggers the deleterious cascade of inflammation and tissue injury associated with hepatic I/R (Figure 13). Thus, mitochondrially-targeted antioxidants such as MitoQ, which appear to be safe in humans and are recently being evaluated for potential therapeutic use [45, 46] (see ClinicalTrials.gov), may represent a promising approach to attenuate the I/R-inflicted liver and most likely other forms of tissue injury, and inflammation.

Acknowledgments

This study was supported by the Intramural Research Program of NIH/NIAAA (to P.P.). Dr. Béla Horváth is a recipient of a Hungarian Research Council Scientific Research Fund Fellowship (OTKA-NKTH-EU MB08-80238). The authors are indebted to Dr. George Kunos, the Scientific Director of NIAAA/NIH for providing key resources and support.

References

1. Jaeschke H. Molecular mechanisms of hepatic ischemia-reperfusion injury and preconditioning. Am J Physiol Gastrointest Liver Physiol. 2003; 284:G15–26. [PubMed: 12488232]
2. Jaeschke H. Reactive oxygen and mechanisms of inflammatory liver injury: Present concepts. J Gastroenterol Hepatol. 2011; 26(Suppl 1):173–179. [PubMed: 21199529]

3. Pacher P, Beckman JS, Liaudet L. Nitric oxide and peroxynitrite in health and disease. Physiol Rev. 2007; 87:315–424. [PubMed: 17237348]
4. Szabo C, Ischiropoulos H, Radi R. Peroxynitrite: biochemistry, pathophysiology and development of therapeutics. Nat Rev Drug Discov. 2007; 6:662–680. [PubMed: 17667957]
5. Szabo C. The pathophysiological role of peroxynitrite in shock, inflammation, and ischemia-reperfusion injury. Shock. 1996; 6:79–88. [PubMed: 8856840]
6. Gero D, Szabo C. Role of the peroxynitrite-poly (ADP-ribose) polymerase pathway in the pathogenesis of liver injury. Curr Pharm Des. 2006; 12:2903–2910. [PubMed: 16918420]
7. Ma TT, Ischiropoulos H, Brass CA. Endotoxin-stimulated nitric oxide production increases injury and reduces rat liver chemiluminescence during reperfusion. Gastroenterology. 1995; 108:463–469. [PubMed: 7835589]
8. Malhi H, Gores GJ, Lemasters JJ. Apoptosis and necrosis in the liver: a tale of two deaths? Hepatology. 2006; 43:S31–44. [PubMed: 16447272]
9. Kim JS, Qian T, Lemasters JJ. Mitochondrial permeability transition in the switch from necrotic to apoptotic cell death in ischemic rat hepatocytes. Gastroenterology. 2003; 124:494–503. [PubMed: 12557154]
10. Levrand S, Vannay-Bouchiche C, Pesse B, Pacher P, Feihl F, Waeber B, Liaudet L. Peroxynitrite is a major trigger of cardiomyocyte apoptosis in vitro and in vivo. Free Radic Biol Med. 2006; 41:886–895. [PubMed: 16934671]
11. Loukili N, Rosenblatt-Velin N, Li J, Clerc S, Pacher P, Feihl F, Waeber B, Liaudet L. Peroxynitrite induces HMGB1 release by cardiac cells in vitro and HMGB1 upregulation in the infarcted myocardium in vivo. Cardiovasc Res. 2011; 89:586–594. [PubMed: 21113057]
12. Castro L, Demicheli V, Tortora V, Radi R. Mitochondrial protein tyrosine nitration. Free Rad Res. 2011; 45:37–52.
13. Moon KH, Hood BL, Mukhopadhyay P, Rajesh M, Abdelmegeed MA, Kwon YI, Conrads TP, Veenstra TD, Song BJ, Pacher P. Oxidative inactivation of key mitochondrial proteins leads to dysfunction and injury in hepatic ischemia reperfusion. Gastroenterology. 2008; 135:1344–1357. [PubMed: 18778711]
14. Chacko BK, Srivastava A, Johnson MS, Benavides GA, Chang MJ, Ye Y, Jhala N, Murphy MP, Kalyanaraman B, Darley-Usmar VM. Mitochondria-targeted ubiquinone (MitoQ) decreases ethanol-dependent micro and macro hepatosteatosis. Hepatology. 2011; 54:153–163. [PubMed: 21520201]
15. Engerson TD, McKelvey TG, Rhyne DB, Boggio EB, Snyder SJ, Jones HP. Conversion of xanthine dehydrogenase to oxidase in ischemic rat tissues. J Clin Invest. 1987; 79:1564–1570. [PubMed: 3294898]
16. Harada H, Hines IN, Flores S, Gao B, McCord J, Scheerens H, Grisham MB. Role of NADPH oxidase-derived superoxide in reduced size liver ischemia and reperfusion injury. Arch Biochem Biophys. 2004; 423:103–108. [PubMed: 14871473]
17. Dorman RB, Wunder C, Saba H, Shoemaker JL, MacMillan-Crow LA, Brock RW. NAD(P)H oxidase contributes to the progression of remote hepatic parenchymal injury and endothelial dysfunction, but not microvascular perfusion deficits. Am J Physiol Gastrointest Liver Physiol. 2006; 290:G1025–1032. [PubMed: 16339298]
18. Abe Y, Hines IN, Zibari G, Pavlick K, Gray L, Kitagawa Y, Grisham MB. Mouse model of liver ischemia and reperfusion injury: method for studying reactive oxygen and nitrogen metabolites in vivo. Free Radic Biol Med. 2009; 46:1–7. [PubMed: 18955130]
19. Batkai S, Osei-Hyiaman D, Pan H, El-Assal O, Rajesh M, Mukhopadhyay P, Hong F, Harvey-White J, Jafri A, Hasko G, Huffman JW, Gao B, Kunos G, Pacher P. Cannabinoid-2 receptor mediates protection against hepatic ischemia/reperfusion injury. FASEB J. 2007; 21:1788–1800. [PubMed: 17327359]
20. Mukhopadhyay P, Rajesh M, Horvath B, Batkai S, Park O, Tanchian G, Gao RY, Patel V, Wink DA, Liaudet L, Hasko G, Mechoulam R, Pacher P. Cannabidiol protects against hepatic ischemia/reperfusion injury by attenuating inflammatory signaling and response, oxidative/nitrative stress, and cell death. Free Rad Biol Med. 2011; 50:1368–1381. [PubMed: 21362471]

21. Dhanasekaran A, Kotamraju S, Karunakaran C, Kalivendi SV, Thomas S, Joseph J, Kalyanaraman B. Mitochondria superoxide dismutase mimetic inhibits peroxide-induced oxidative damage and apoptosis: role of mitochondrial superoxide. Free Radic Biol Med. 2005; 39:567–583. [PubMed: 16085176]
22. Smith RA, Hartley RC, Murphy MP. Mitochondria-Targeted Small Molecule Therapeutics and Probes. Antioxid Redox Signal. 2011; 15(12):3021–3038. [PubMed: 21395490]
23. Smith RA, Murphy MP. Mitochondria-targeted antioxidants as therapies. Discov Med. 2011; 11:106–114. [PubMed: 21356165]
24. Smith RA, Hartley RC, Cocheme HM, Murphy MP. Mitochondrial pharmacology. Trends Pharmacol Sci. 2012 in press.
25. Batkai S, Mukhopadhyay P, Horvath B, Rajesh M, Gao RY, Mahadevan A, Amere M, Battista N, Lichtman AH, Gauson LA, Maccarrone M, Pertwee RG, Pacher P. Delta8-Tetrahydrocannabivarin prevents hepatic ischaemia/reperfusion injury by decreasing oxidative stress and inflammatory responses through cannabinoid CB2 receptors. Br J Pharmacol. 2012; 165:2450–2461. [PubMed: 21470208]
26. Horvath B, Magid L, Mukhopadhyay P, Batkai S, Rajesh M, Park O, Tanchian G, Gao RY, Goodfellow CE, Glass M, Mechoulam R, Pacher P. A new cannabinoid CB2 receptor agonist HU-910 attenuates oxidative stress, inflammation and cell death associated with hepatic ischaemia/reperfusion injury. Br J Pharmacol. 2012; 165:2462–2478. [PubMed: 21449982]
27. Cassina P, Cassina A, Pehar M, Castellanos R, Gandelman M, de Leon A, Robinson KM, Mason RP, Beckman JS, Barbeito L, Radi R. Mitochondrial dysfunction in SOD1G93A-bearing astrocytes promotes motor neuron degeneration: prevention by mitochondrial-targeted antioxidants. J Neurosci. 2008; 28:4115–4122. [PubMed: 18417691]
28. Mukhopadhyay P, Horvath B, Zsengeller Z, Zielonka J, Tanchian G, Holovac E, Kechrid M, Patel V, Stillman IE, Parikh SM, Joseph J, Kalyanaraman B, Pacher P. Mitochondrial-targeted antioxidants represent a promising approach for prevention of cisplatin-induced nephropathy. Free Radic Biol Med. 2012; 52(2):497–506. [PubMed: 22120494]
29. Mukhopadhyay P, Rajesh M, Pan H, Patel V, Mukhopadhyay B, Batkai S, Gao B, Hasko G, Pacher P. Cannabinoid-2 receptor limits inflammation, oxidative/nitrosative stress, and cell death in nephropathy. Free Radic Biol Med. 2010; 48:457–467. [PubMed: 19969072]
30. Horvath B, Mukhopadhyay P, Kechrid M, Patel V, Tanchian G, Wink DA, Gertsch J, Pacher P. beta-Caryophyllene ameliorates cisplatin-induced nephrotoxicity in a cannabinoid 2 receptor-dependent manner. Free Radic Biol Med. 2012; 52:1325–1333. [PubMed: 22326488]
31. Hornig-Do HT, Gunther G, Bust M, Lehnartz P, Bosio A, Wiesner RJ. Isolation of functional pure mitochondria by superparamagnetic microbeads. Anal Biochem. 2009; 389:1–5. [PubMed: 19285029]
32. Mukhopadhyay P, Horvath B, Rajesh M, Matsumoto S, Saito K, Batkai S, Patel V, Tanchian G, Gao RY, Cravatt BF, Hasko G, Pacher P. Fatty acid amide hydrolase is a key regulator of endocannabinoid-induced myocardial tissue injury. Free Radic Biol Med. 2011; 50:179–195. [PubMed: 21070851]
33. Mukhopadhyay P, Rajesh M, Batkai S, Patel V, Kashiwaya Y, Liaudet L, Evgenov OV, Mackie K, Hasko G, Pacher P. CB1 cannabinoid receptors promote oxidative stress and cell death in murine models of doxorubicin-induced cardiomyopathy and in human cardiomyocytes. Cardiovasc Res. 2010; 85:773–784. [PubMed: 19942623]
34. Mukhopadhyay P, Rajesh M, Batkai S, Kashiwaya Y, Hasko G, Liaudet L, Szabo C, Pacher P. Role of superoxide, nitric oxide, and peroxynitrite in doxorubicin-induced cell death in vivo and in vitro. Am J Physiol Heart Circ Physiol. 2009; 296:H1466–1483. [PubMed: 19286953]
35. Jaeschke H, Ramachandran A. Reactive oxygen species in the normal and acutely injured liver. J Hepatol. 2011; 55:227–228. [PubMed: 21238521]
36. Jaeschke H. Role of reactive oxygen species in hepatic ischemia-reperfusion injury and preconditioning. J Invest Surg. 2003; 16:127–140. [PubMed: 12775429]
37. Peglow S, Toledo AH, Anaya-Prado R, Lopez-Neblina F, Toledo-Pereyra LH. Allopurinol and xanthine oxidase inhibition in liver ischemia reperfusion. J Hepatobiliary Pancreat Sci. 2010

38. Pacher P, Nivorozhkin A, Szabo C. Therapeutic effects of xanthine oxidase inhibitors: renaissance half a century after the discovery of allopurinol. Pharmacological reviews. 2006; 58:87–114. [PubMed: 16507884]

39. Lee VG, Johnson ML, Baust J, Laubach VE, Watkins SC, Billiar TR. The roles of iNOS in liver ischemia-reperfusion injury. Shock. 2001; 16:355–360. [PubMed: 11699073]

40. Beckman JS, Koppenol WH. Nitric oxide, superoxide, and peroxynitrite: the good, the bad, and ugly. Am J Physiol. 1996; 271:C1424–1437. [PubMed: 8944624]

41. Jaeschke H, Lemasters JJ. Apoptosis versus oncotic necrosis in hepatic ischemia/reperfusion injury. Gastroenterology. 2003; 125:1246–1257. [PubMed: 14517806]

42. Dikalov S. Cross talk between mitochondria and NADPH oxidases. Free Radic Biol Med. 2011; 51:1289–1301. [PubMed: 21777669]

43. Tsung A, Klune JR, Zhang X, Jeyabalan G, Cao Z, Peng X, Stolz DB, Geller DA, Rosengart MR, Billiar TR. HMGB1 release induced by liver ischemia involves Toll-like receptor 4 dependent reactive oxygen species production and calcium-mediated signaling. J Exp Med. 2007; 204:2913–2923. [PubMed: 17984303]

44. Gill R, Tsung A, Billiar T. Linking oxidative stress to inflammation: Toll-like receptors. Free Radic Biol Med. 2010; 48:1121–1132. [PubMed: 20083193]

45. Gane EJ, Weilert F, Orr DW, Keogh GF, Gibson M, Lockhart MM, Frampton CM, Taylor KM, Smith RA, Murphy MP. The mitochondria-targeted anti-oxidant mitoquinone decreases liver damage in a phase II study of hepatitis C patients. Liver Int. 2010; 30:1019–1026. [PubMed: 20492507]

46. Snow BJ, Rolfe FL, Lockhart MM, Frampton CM, O'Sullivan JD, Fung V, Smith RA, Murphy MP, Taylor KM. A double-blind, placebo-controlled study to assess the mitochondria-targeted antioxidant MitoQ as a disease-modifying therapy in Parkinson's disease. Mov Disord. 2010; 25:1670–1674. [PubMed: 20568096]

Highlights

- Ischemia-reperfusion (I/R) injury is a pivotal mechanism of organ damage/dysfunction
- The exact role and time of mitochondrial oxidants generation in liver I/R is elusive
- Mitochondrial oxidants generation triggers I/R-induced liver inflammation and injury
- Mitochondrial antioxidants (MTAs) prevent the I/R-induced oxidative/nitrative injury
- MTAs prevent the I/R-induced acute/delayed inflammatory response and cell death

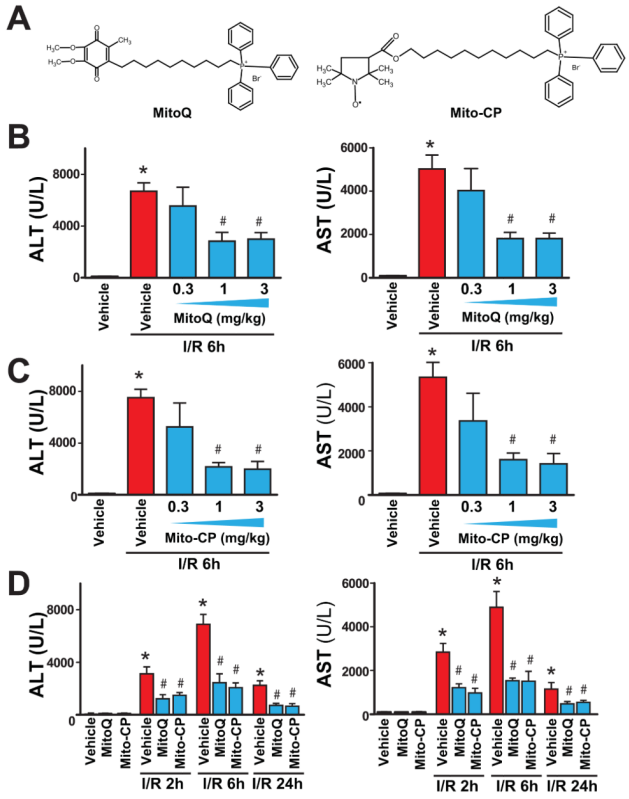

Figure 1. MitoQ and Mito-CP pretreatment dose-dependently attenuates hepatic I/R injury

Panel A: Chemical structures of MitoQ and Mito-CP.

Panels B and C: Serum transaminases ALT and AST levels in sham-operated mice treated with vehicle or in mice exposed to 1 h of hepatic ischemia followed by 6 h of reperfusion (I/R 6h) pretreated with vehicle, MitoQ or Mito-CP (0.3, 1 and 3 mg/kg i.p., n=6–21/group).

Panel D: Serum ALT and AST levels in sham operated mice treated with vehicle, MitoQ or Mito-CP (n=6–21/group) or in mice exposed to 1 h of hepatic ischemia followed by 2, 6 and 24 hours of reperfusion (I/R 2h, 6 h and 24h) pretreated with vehicle or MitoQ/Mito-CP (3 mg/kg i.p.). The peak damaged occurs at I/R 6h, and MitoQ/Mito-CP is able to attenuate the inflicted injury at any point investigated. *P<0.05 sham control vs. I/R; #P<0.05 I/R vs. corresponding I/R+ MitoQ/Mito-CP.

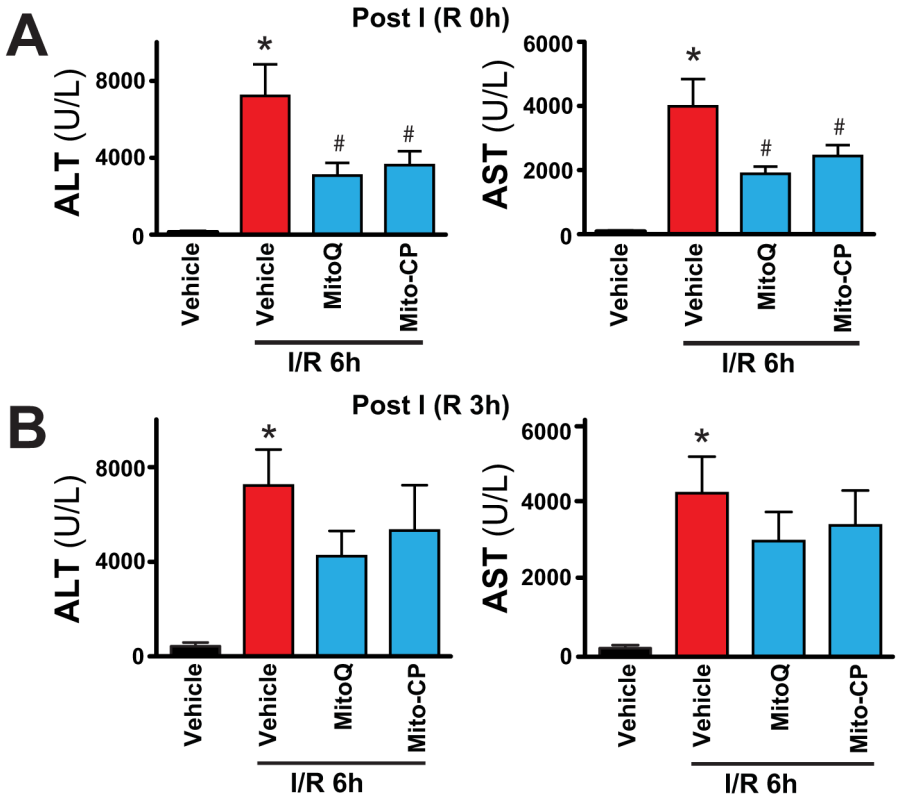

Figure 2. MitoQ and Mito-CP treatment after ischemia attenuates hepatic I/R injury

Panels A and B: Serum transaminases ALT and AST levels in sham-operated mice or in mice exposed to 1 h of hepatic ischemia followed by 6 h of reperfusion (I/R 6h) treated with vehicle or MitoQ/Mito-CP (3 mg/kg i.p., n=6–10/group) right after the ischemia before the reperfusion (post I (R 0h)) or 3 hours following the ischemia (post I (R 3h)), respectively. *P<0.05 sham control vs. I/R; #P<0.05 I/R vs. corresponding I/R+ MitoQ/Mito-CP. Notably, MitoQ/Mito-CP are able to attenuate the inflicted injury only when administered right after the ischemia, but not 3 hours after.

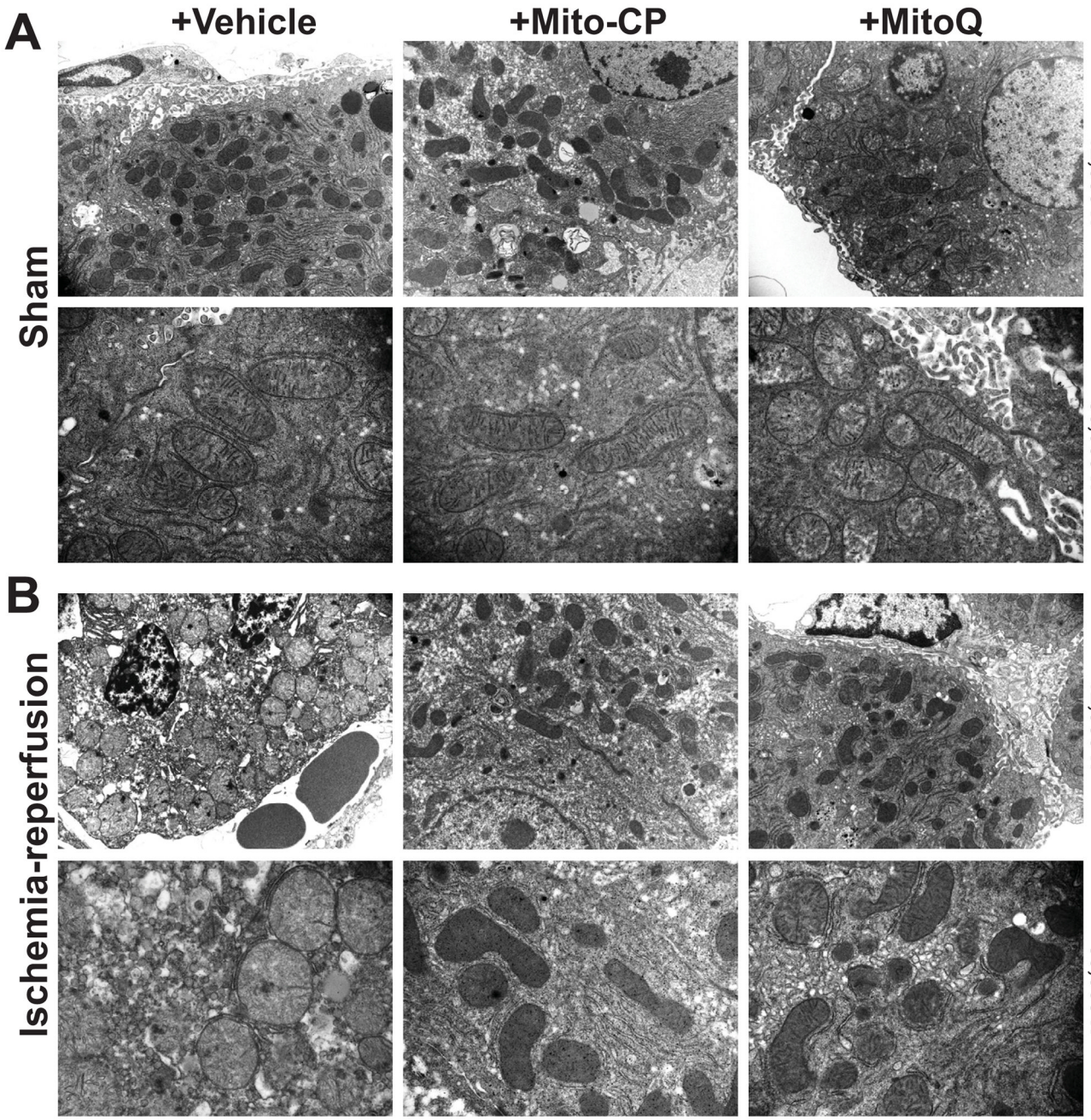

Figure 3. MitoQ and Mito-CP treatment attenuates I/R injury-induced early mitochondrial injury

Panel A: Representative transmission electron micrographs of the non-ischemic control livers of mice undergoing sham surgery (sham) treated with vehicle reveal normal hepatic tissue with good preservation of hepatocytes and lining cells of sinusoidal venules, as well as normal mitochondrial structure, which are not affected by treatments with MitoQ/Mito-CP (3 mg/kg i.p.). Upper images depict 12,000× and lower 30,000× magnification.

Panel B: Post-ischemic liver tissue at 2 hours of reperfusion (I/R 2h) exhibit marked disintegration of ultrastructure (e.g., swelling of mitochondria, vacuolization, nuclear and cytoplasmic degeneration) in most hepatocytes. In some mitochondria the matrix totally

disappears and only the outer membrane remains, while in others, the cristae are disorganized because of edema in the matrix (left images). Mito-CP/MitoQ pretreatment (3 mg/kg i.p.) markedly attenuates the morphological and mitochondrial injury induced by 1 h of ischemia followed by 2 hours of reperfusion (I/R 2h) to a similar extent (middle and right panels). Upper images depict 12,000× and lower 30,000× magnification. A similar histological profile was seen in three to five livers/group.

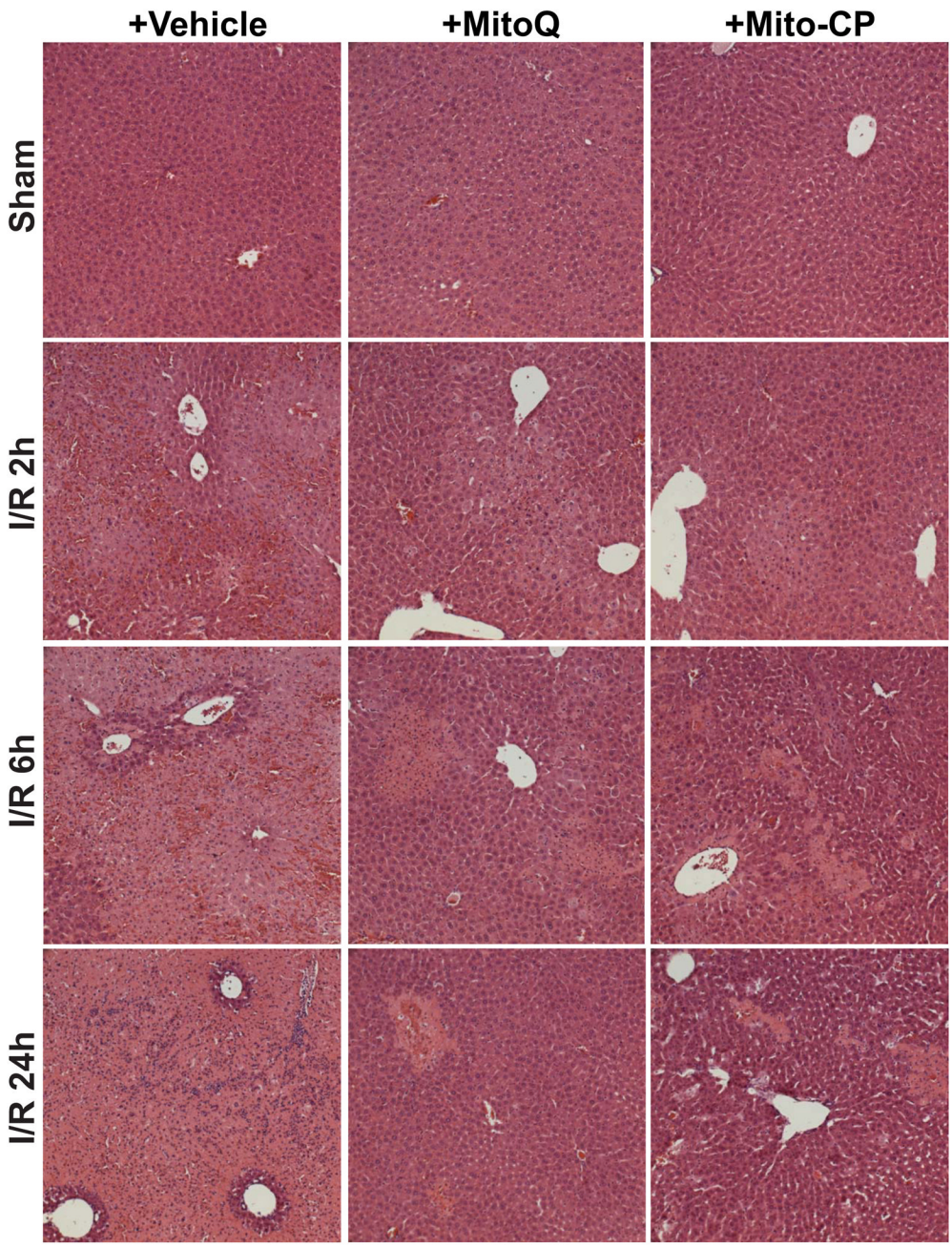

Figure 4. MitoQ and Mito-CP treatment attenuates histological damage at 2, 6 and 24h of reperfusion following 1 hour of ischemia

Hematoxylin and eosin staining of representative liver sections of sham mice treated with vehicle (sham), and mice exposed to 1 hour of ischemia followed by 2, 6 or 24h of reperfusion treated with vehicle or Mito-CP/MitoQ (3 mg/kg i.p.). I/R inflicts marked coagulation necrosis in the liver (lighter staining at 6 and 24 h of reperfusion), which is markedly attenuated by MitoQ/Mito-CP pretreatment. MitoQ/Mito-CP has no effect in control mice exposed to sham surgery. Figure 4 depicts 200x magnification. A similar histological profile was seen in three to five livers/group.

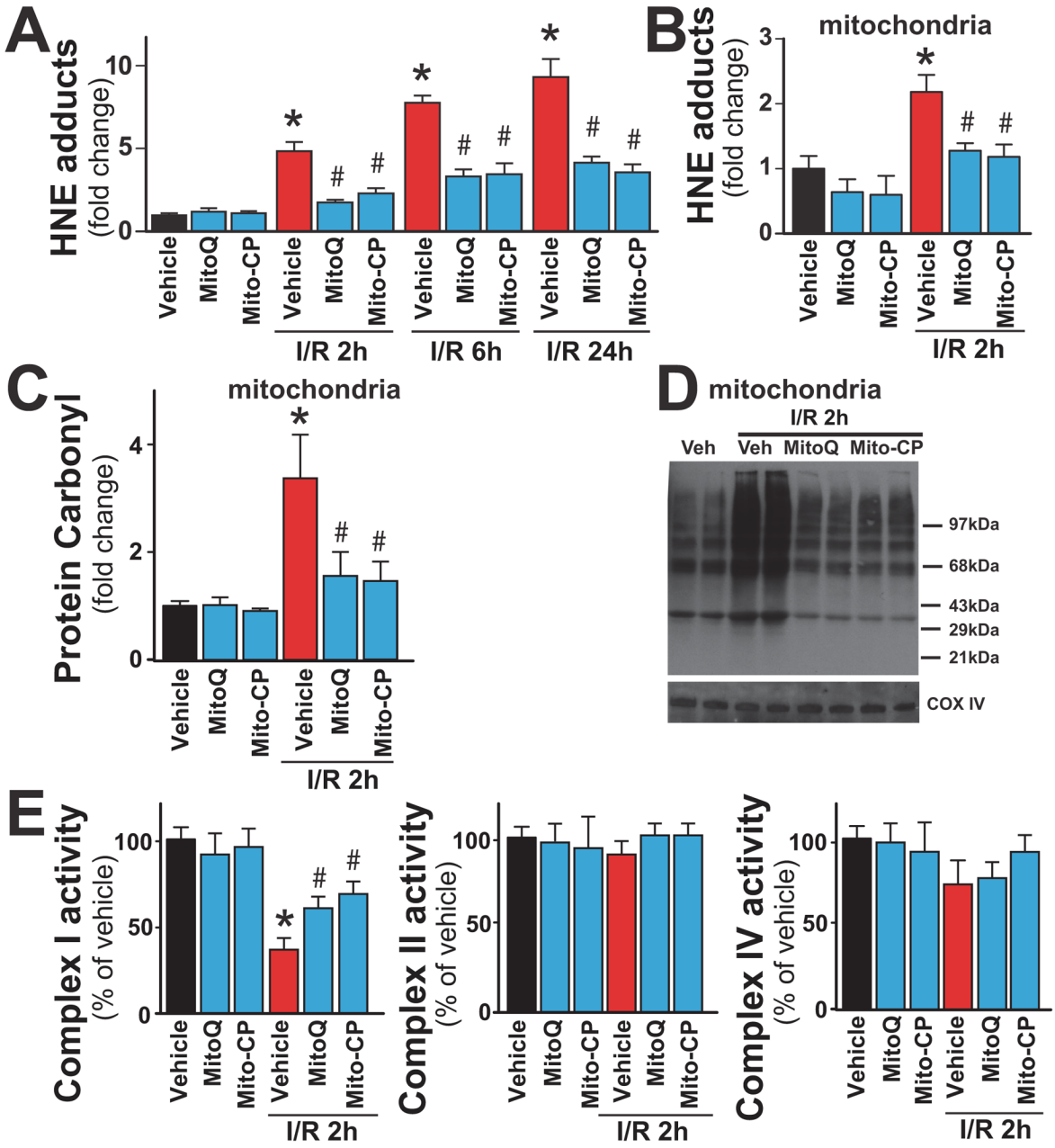

Figure 5. MitoQ and Mito-CP treatment attenuates the I/R-induced increased hepatic and/or mitochondrial oxidative stress and dysfunction

Panels A: HNE adducts (a marker for lipid peroxidation/oxidative stress) are time-dependently increased following I/R injury peaking at 24 hours. MitoQ/Mito-CP pretreatment (3 mg/kg i.p.) attenuates these increases.

Panel B: HNE adducts in mitochondrial fraction are increased following I/R 2h and are attenuated with MitoQ/Mito-CP pretreatment (3 mg/kg i.p.).

Panels C, D: Carbonyl adducts in mitochondrial fraction measured by ELISA or Oxyblot are increased following I/R 2h and are attenuated with MitoQ/Mito-CP pretreatment (3 mg/kg i.p.), respectively.

Panel E: The complex I activity in isolated liver mitochondria is markedly decreased following I/R 2h, which is attenuated with MitoQ/Mito-CP pretreatment (3 mg/kg i.p.). *P<0.05 sham control vs. I/R; #P<0.05 I/R vs. corresponding I/R+MitoQ/Mito-CP. For panels A–C and E n=6–12/group.

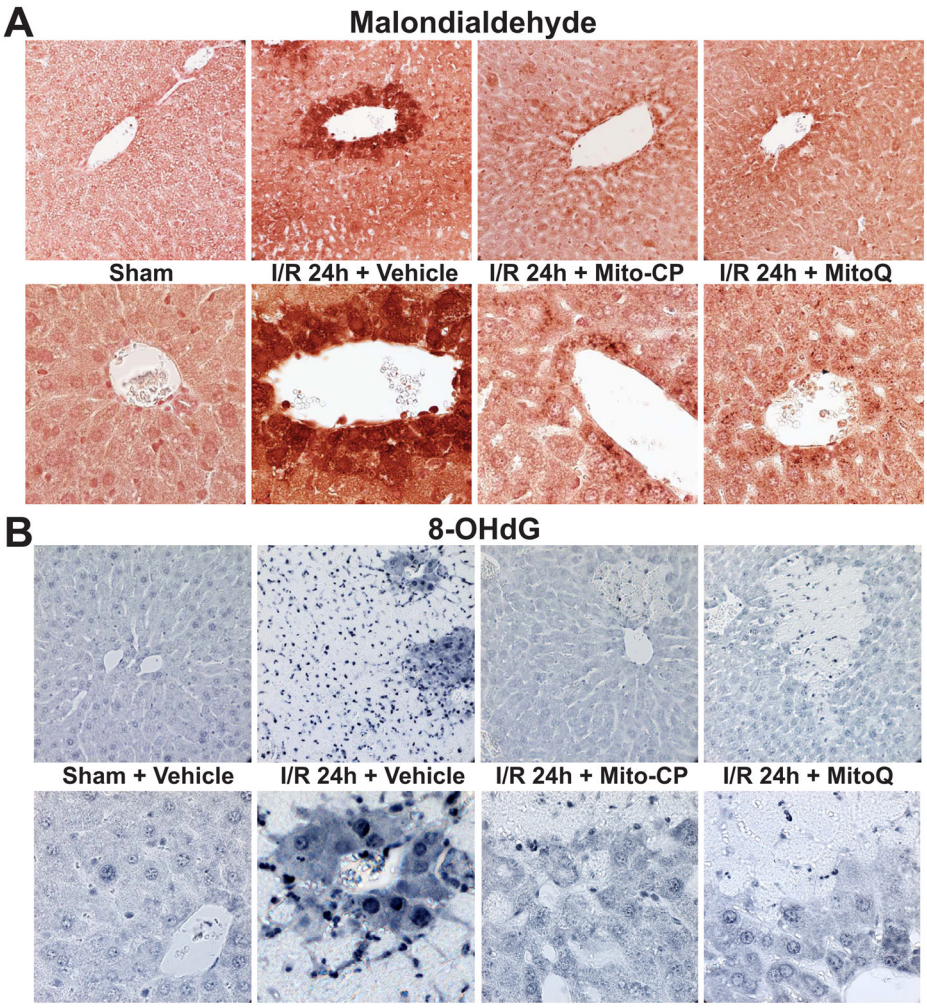

Figure 6. MitoQ and Mito-CP treatment attenuates the I/R-induced increased hepatic malondialdehyde formation and oxidative DNA damage

Panel A: Malondialdehyde staining (brown; a marker of lipid peroxidation/oxidative stress) of representative liver sections of sham mice treated with vehicle (sham) or MitoQ/Mito-CP (antioxidants in sham mice had no effects, not shown), and mice exposed to 1 hour of ischemia followed by 24 hours of reperfusion (I/R 24h) treated with vehicle or MitoQ/Mito-CP (3 mg/kg i.p.). 24 hours of I/R triggers marked increase in liver malondialdehyde formation, which is predominantly localized to endothelial cells, perivascular hepatocytes, and infiltrating (or attached to the endothelium) inflammatory cells, and these increases are markedly attenuated by pretreatment with MitoQ/Mito-CP. Minimal staining is seen in the livers of control mice exposed to sham surgery. Slides are counterstained by nuclear fast red. Upper row of images depicts 400× magnification, while the lower one 1000× magnification. A similar histological profile was seen in three to five livers/group.

Panel B: 8-OHdG staining (blue; marker of oxidative DNA damage) of representative liver sections of sham mice treated with vehicle (sham) or MitoQ/Mito-CP (antioxidants in sham mice had no effects, not shown) and mice exposed to 1 hour of ischemia followed by 24 hours of reperfusion (I/R 24h) treated with vehicle or MitoQ/Mito-CP. 24 hours of I/R triggers markedly increased 8-OHdG formation in endothelial cells, perivascular hepatocytes and infiltrating inflammatory cells, and these changes are attenuated by pretreatment with MitoQ/Mito-CP. Please note that the necrotic areas are lighter and

infiltrated by neutrophils showing intense nuclear staining. Minimal nuclear 8-OHdG staining is seen in the livers of control mice exposed to sham surgery. Upper row of images depicts 400× magnification, while the lower one 1000× magnification. A similar histological profile was seen in three to five livers/group.

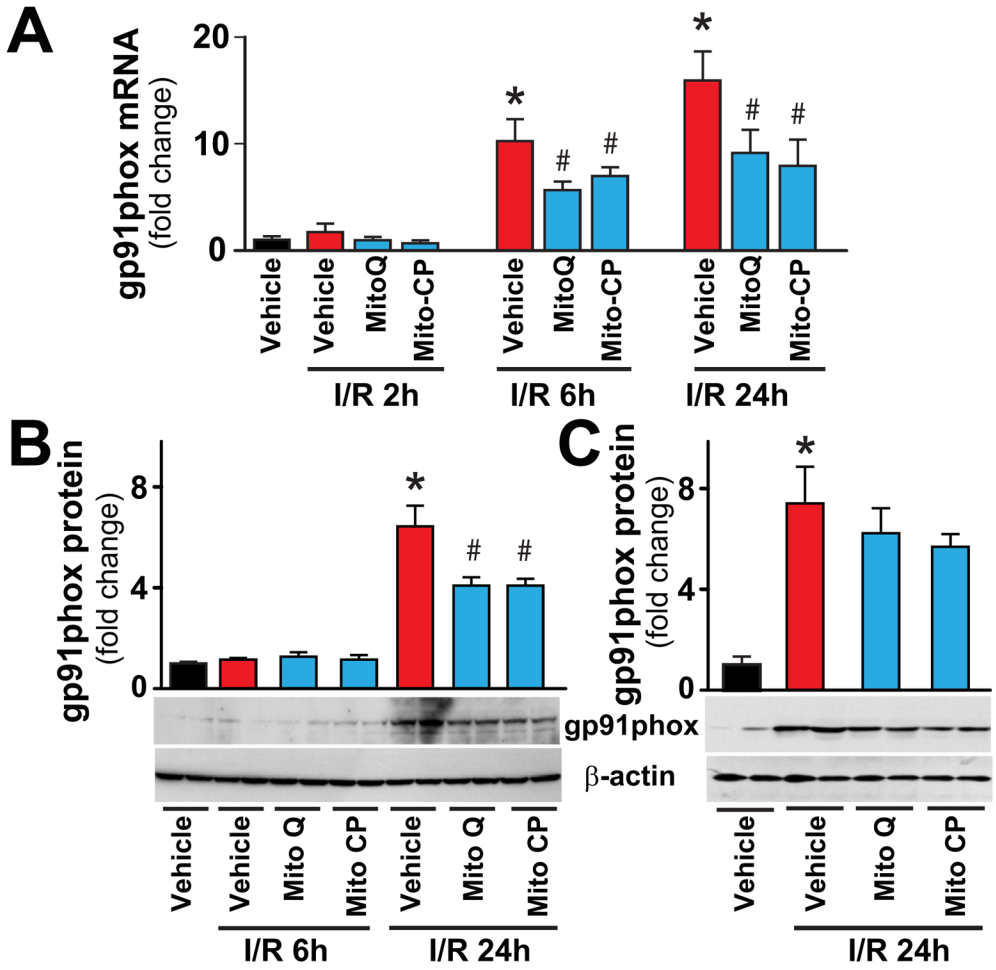

Figure 7. MitoQ and Mito-CP treatment attenuates the I/R-induced gp91phox expression

Panels A–C: Real-time PCR and Western blot show significant increase in hepatic NAD(P)H oxidase isoform NOX2/gp91phox mRNA or protein expression level at 24h of reperfusion (I/R 24h). Pretreatment with MitoQ/Mito-CP (Panels A and B), but not post-treatment following 3 hours of reperfusion (Panel C), attenuates the I/R-induced increases. n=6–14/group. *P<0.05 sham control vs. I/R; #P<0.05 I/R vs. corresponding I/R+MitoQ/Mito-CP.

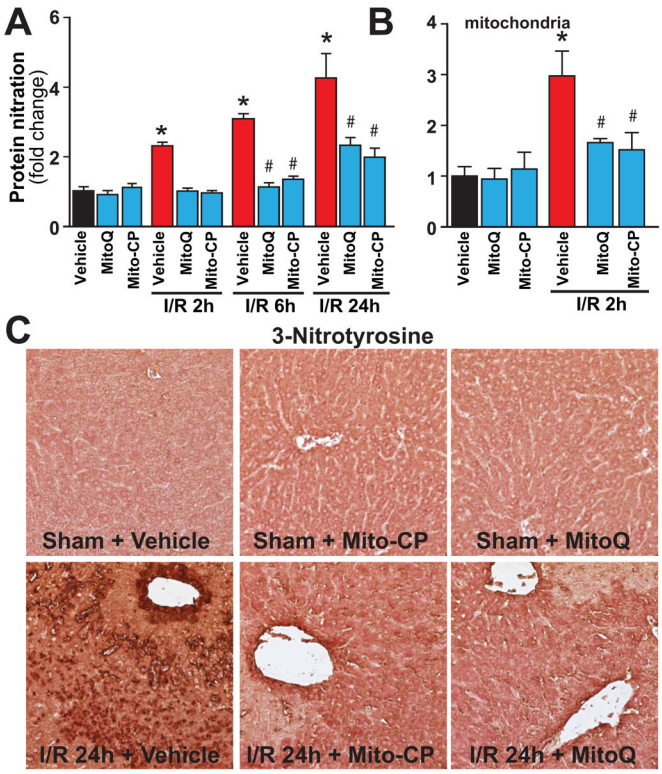

Figure 8. MitoQ and Mito-CP treatment attenuates the I/R-induced increased nitrative stress

Panel A: Protein nitration (3-NT), a marker for nitrative stress, time-dependently increases following I/R injury peaking at 24 hours. MitoQ/Mito-CP pretreatment (3 mg/kg i.p.) attenuates this increase. n=8–12/group. *P<0.05 sham control vs. I/R; #P<0.05 I/R vs. corresponding I/R+MitoQ/Mito-CP.

Panel B: Protein nitration in mitochondria is increased at I/R 2h. MitoQ/Mito-CP pretreatment (3 mg/kg i.p.) attenuates this increase. n=4–8/group. *P<0.05 sham control vs. I/R; #P<0.05 I/R vs. corresponding I/R+MitoQ/Mito-CP.

Panel C: 3-Nitrotyrosine staining (brown) of representative liver sections of sham mice treated with vehicle (sham), MitoQ/Mito-CP and mice exposed to 1 hour of ischemia followed by 24 hours of reperfusion (I/R 24h) treated with vehicle or MitoQ/Mito-CP. Images depicts 400× magnification. A similar histological profile was seen in three to five livers/group.

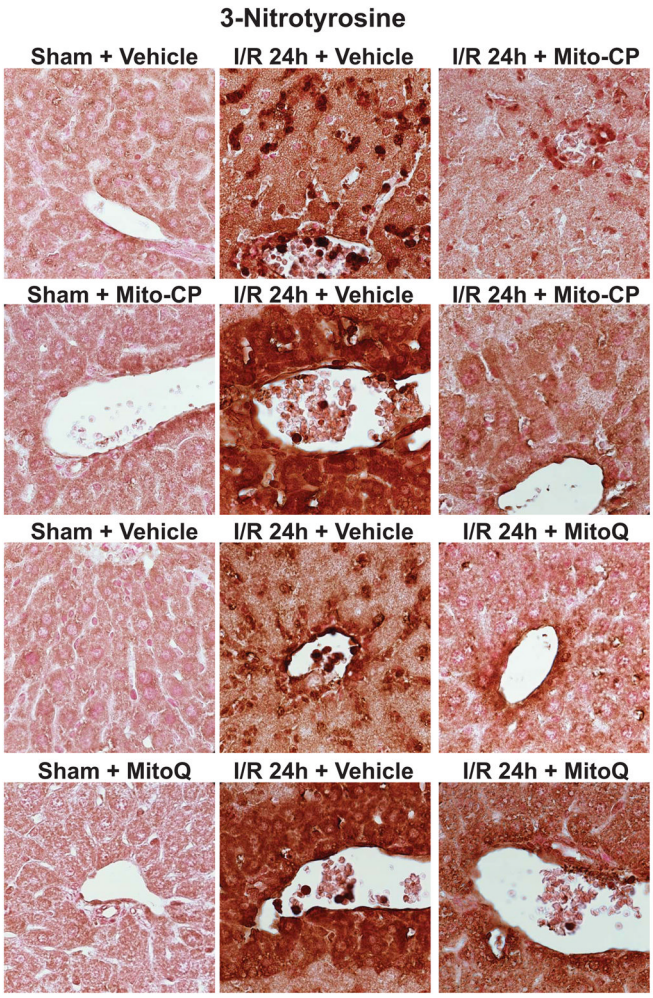

Figure 9. MitoQ and Mito-CP treatment attenuates the I/R-induced increased nitrative stress in hepatocytes, endothelial and inflammatory cells

3-Nitrotyrosine staining of representative liver sections of sham mice treated with vehicle (sham), MitoQ/Mito-CP and mice exposed to 1 hour of ischemia followed by 24 hours of reperfusion treated with vehicle (I/R 24h) or MitoQ/Mito-CP. 24 hours of I/R (middle images) triggers markedly increased 3-NT formation in endothelial cells, perivascular hepatocytes and infiltrating inflammatory cells, and these changes are attenuated by pretreatment with MitoQ/Mito-CP. Images depict 1000× magnification. A similar histological profile was seen in three to five livers/group.

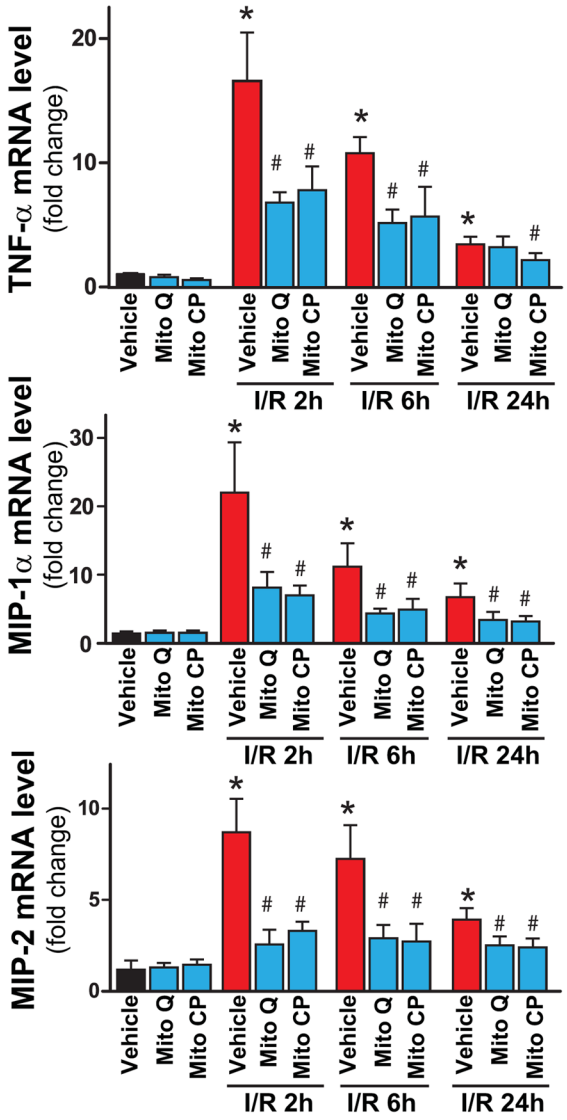

Figure 10. MitoQ and Mito-CP treatment attenuate the I/R-induced increased acute pro-inflammatory response

Real-time PCR shows significant increase in hepatic pro-inflammatory cytokine TNF-α, chemokines MIP-1α and MIP-2 mRNA levels at 2h of reperfusion (I/R 2h), and a gradual decrease by 24 hours (I/R 24h). Pretreatment with MitoQ/Mito-CP (3 mg/kg i.p.) attenuates the I/R-induced increased levels of cytokines/chemokines. n=7–12/group. *P<0.05 sham control vs. I/R; #P<0.05 I/R vs. corresponding I/R+MitoQ/Mito-CP.

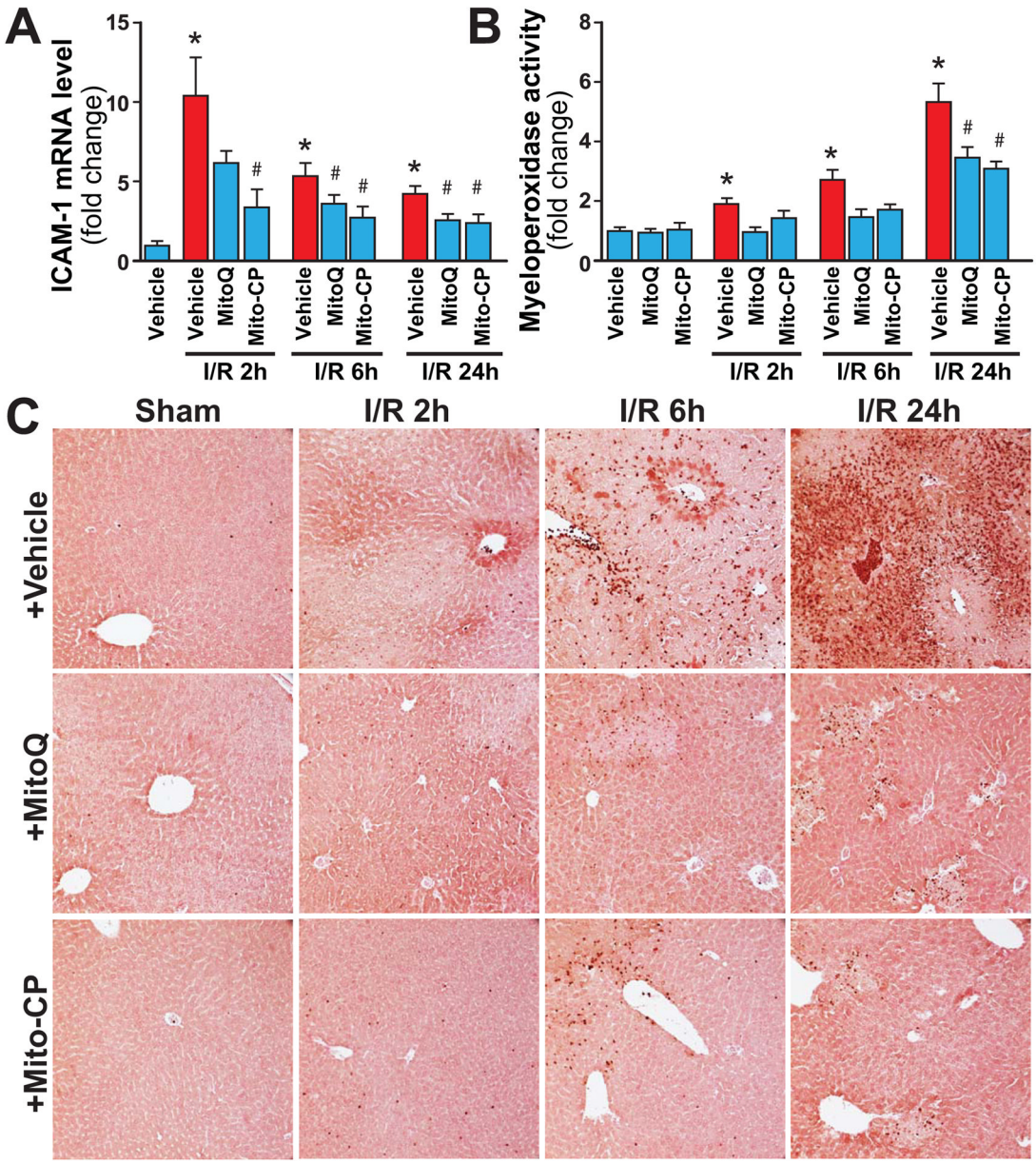

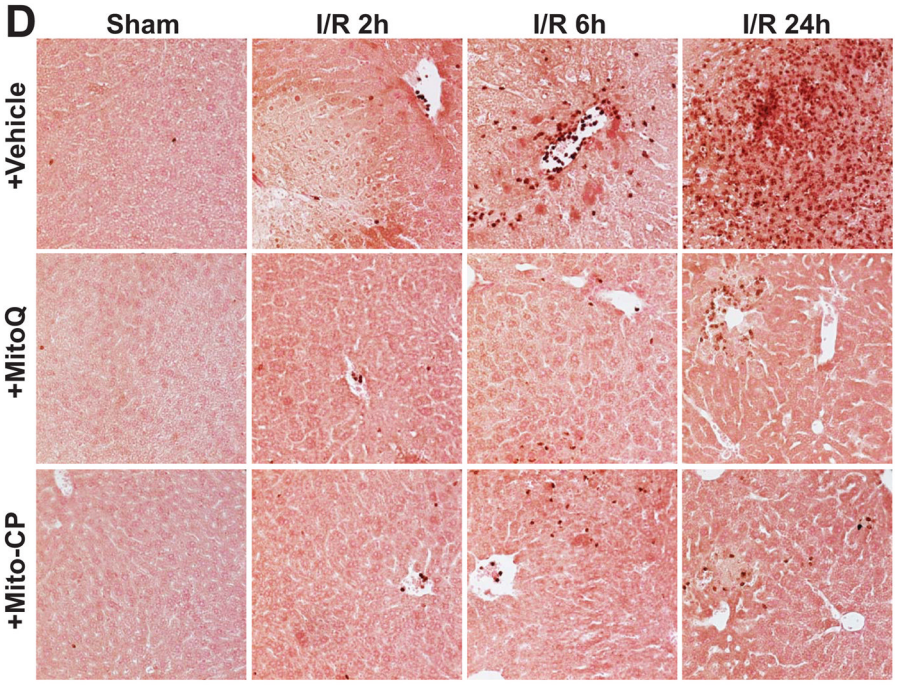

Figure 11. MitoQ and Mito-CP treatment attenuates the I/R-induced increased adhesion molecule expression and enhanced delayed neutrophil infiltration in the liver

Panel A: Real-time PCR shows significant increase in hepatic adhesion molecule ICAM-1 mRNA level at 2h of reperfusion (I/R 2h), and a gradual decrease by 24 hours (I/R 24h). Pretreatment with MitoQ/Mito-CP (3 mg/kg i.p.) significantly attenuates the I/R-induced increased level of adhesion molecule. n=7–12/group. *P<0.05 sham control vs. I/R; #P<0.05 I/R vs. corresponding I/R+MitoQ/Mito-CP.

Panel B: Quantification of MPO activity from the liver extracts shows significant time-dependent increases associated with I/R (peaking at I/R 24h), which are attenuated by pretreatment with MitoQ/Mito-CP (3 mg/kg i.p.). n=8–12/group. *P<0.05 sham control vs. I/R; #P<0.05 I/R vs. corresponding I/R+MitoQ/Mito-CP.

Panel C–D: Myeloperoxidase (MPO) staining (brown) of representative liver sections of sham mice treated with vehicle (sham) or MitoQ/Mito-CP, and mice exposed to 1 hour of ischemia followed by 2, 6 or 24 hours of reperfusion treated with vehicle or MitoQ/Mito-CP. These images reveal increased neutrophils attachment to the endothelium and accumulation in the vessels at I/R 6h followed by marked infiltration of liver tissue at I/R 24h. Pretreatment with MitoQ/Mito-CP (3 mg/kg i.p.) attenuates the I/R-induced increased neutrophil infiltration. Slides were counterstained by nuclear fast red. Panel C images depict 200× magnification, while Panel D depicts 400× magnification. A similar histological profile was seen in three to five livers/group.

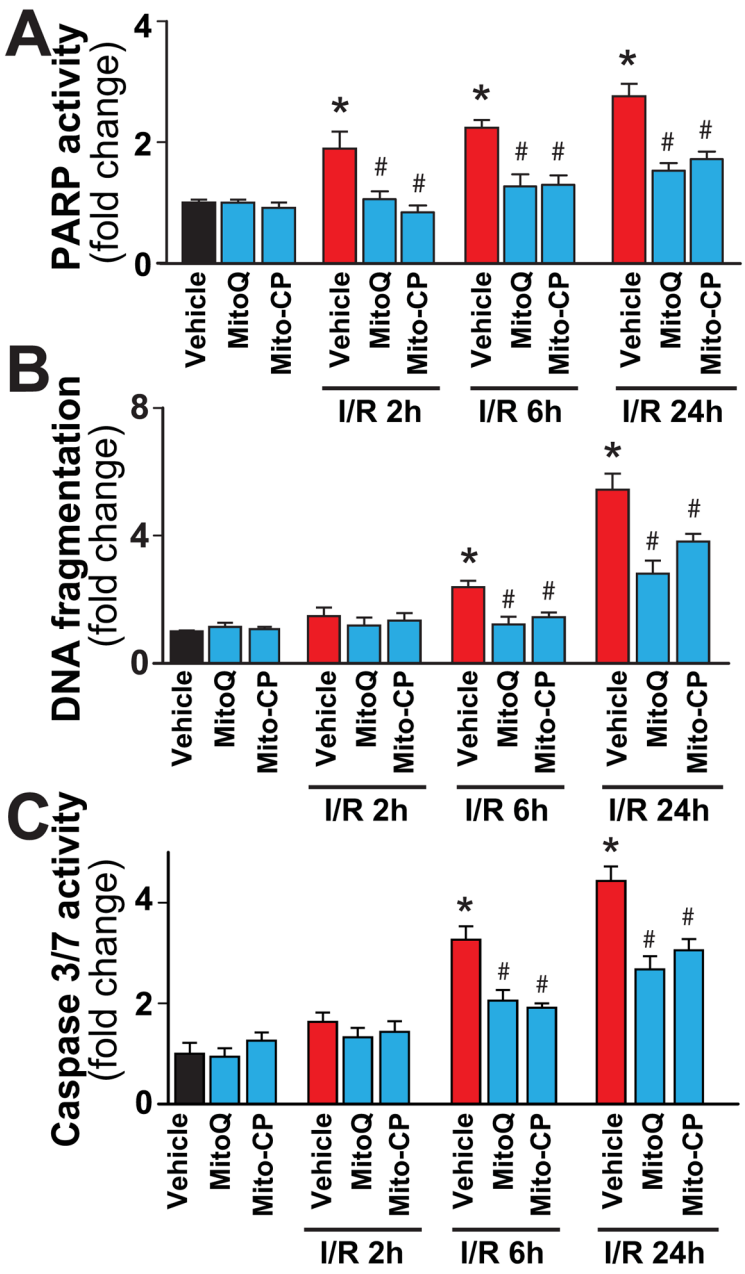

Figure 12. MitoQ and Mito-CP treatment attenuates the I/R-induced increased cell death

Panel A: PARP activity, a marker for cell death (mostly necrotic) increases at 2, 6 and 24 h of I/R. MitoQ/Mito-CP pretreatment (3 mg/kg i.p.) attenuates these increases.

Panels B and C: DNA fragmentation and caspase 3/7 activity (markers of apoptotic cell death) increase only from 6 h of I/R peaking at 24 hours. MitoQ/Mito-CP pretreatment (3 mg/kg i.p.) attenuates these increases. n=8–13/group. *P<0.05 sham control vs. I/R; #P<0.05 I/R vs. corresponding I/R+MitoQ/Mito-CP.

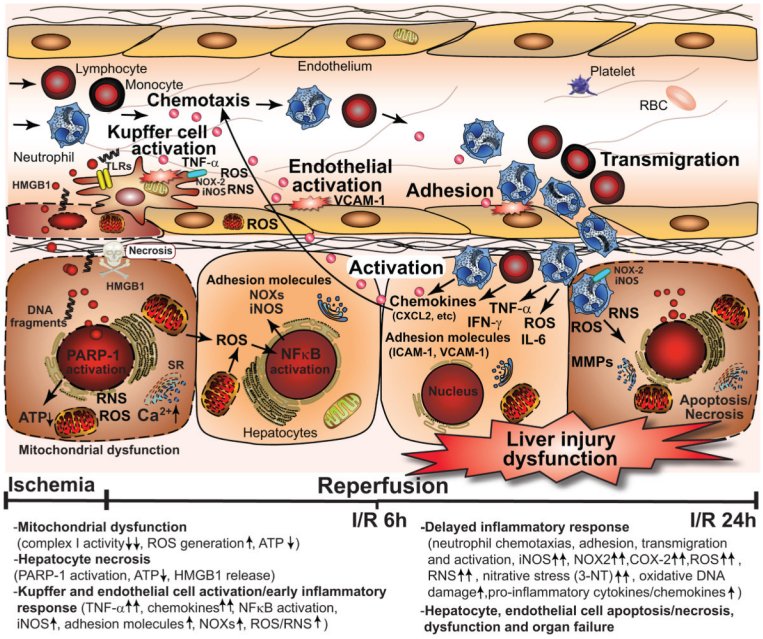

Figure 13. Simplified mechanisms of the interplay of mitochondrial dysfunction and oxidative stress with inflammatory responses and cell death during hepatic ischemia-reperfusion (I/R) injury

The metabolic stress during ischemia and initial phase of reperfusion leads to mitochondrial dysfunction in hepatocytes and sinusoidal endothelial cells, increased mitochondrial reactive oxygen (e.g. superoxide and hydrogen peroxide) and nitrogen species (e.g. peroxynitrite) formation (ROS/RNS), Ca^{2+} accumulation, and activation of various necrotic cell death pathways by ROS/RNS, such as poly(ADP)-ribose polymerase 1 (PARP-1), which leads to ATP depletion and early cell necrosis. Superoxide may also readily react with nitric oxide (NO) during early hepatic reperfusion (the latter can be derived from nitric oxide synthases, most likely iNOS via a diffusion limited reaction to form a more potent oxidant peroxynitrite, further impairing mitochondrial and cellular functions and increasing ROS generation. Hepatic I/R also attenuates endothelial NO synthase activity in sinusoidal endothelial cells during I/R leading to endothelial dysfunction, favoring sinusoidal vasoconstriction and secondary ischemic injury. Necrotic hepatocytes and endothelial cells release various damage-associated molecular patterns (e.g. high mobility group box 1 protein (HMGB1), DNA fragments, and lipid peroxidation products such as hydroxynonenal (HNE), among others), which activate Kupffer cells (the resident macrophages of the liver) via several toll like receptors (TLRs) in a nuclear factor kappa B (NFκB)-dependent manner. The activated Kupffer cells subsequently produce numerous pro-inflammatory cytokines and chemokines such as tumor necrosis factor α (TNF-α), macrophage inflammatory proteins (MIP1/2), and additional ROS and nitric oxide (NO) through the increased expression of ROS generating NAD(P)H oxidase isoform NOX-2 and inducible nitric oxide synthase (iNOS), further fueling oxidative/nitrative injury and priming/chemotaxis of various inflammatory cells. The initial oxidant-induced injury also leads to the activation of endothelial cells which in concert with activated Kupffer cells and certain subtypes of T lymphocytes orchestrate the acute and delayed pro-inflammatory response leading to attraction of neutrophils and other inflammatory cells into the damaged tissue upon late reperfusion. These inflammatory cells further release oxidants and proteolytic enzymes enhancing intracellular oxidative/nitrative stress and mitochondrial dysfunction in hepatocytes, thereby promoting apoptotic and/or necrotic forms of cell demise.